A Look at Membrane Patches with a Scanning Force Microscope

J. K. Heinrich Hörber,* Johannes Mosbacher,‡ Walter Häberle,§ J. Peter Ruppersberg,¶ and Bert Sakmann‡
*European Molecular Biology Laboratory, 69117 Heidelberg, Germany; ‡Max-Planck-Institut für medizinische Forschung, 69120 Heidelberg, Germany; §IBM Physik Gruppe, 80799 München, Germany; and ¶Hals-Nasen-Ohren Klinik, Universität Tübingen, 72076 Tübingen, Germany

ABSTRACT   We combined scanning force microscopy with patch-clamp techniques in the same experimental setup and obtained images of excised membrane patches spanning the tip of a glass pipette. These images indicate that cytoskeleton structures are still present in such membrane patches and form a strong connection between the membrane and the glass wall. This gives the membrane patch the appearance of a tent, stabilized by a scaffold of ropes. The lateral resolution of the images depends strongly on the observed structures and can reach values as low as 10 nm on the cytoskeleton elements of a (inside-out) patch. The observations suggest that measurements of membrane elasticity can be made, opening the way for further studies on mechanical properties of cell membranes.

INTRODUCTION

An obvious research area for a surface science instrument like the scanning force microscope (SFM) in biology is the investigation of cell membrane surfaces (Häberle et al., 1989; Henderson et al., 1992; Hoh et al., 1992; Radmacher et al., 1992; Chang et al., 1993; Le Grimellec et al., 1994). The importance of this SFM application is emphasized by the basic role of cell membranes in intercellular interactions and in regulation of intracellular processes.

One of the major features of cell membranes is the process of selective transmembrane transport, like endo- and exocytosis and the flow of ions. The latter is actively regulated by membrane proteins, called ion channels. Properties of ion channels are measured by recording transmembrane currents using the patch-clamp technique (PCT). The current through a single channel is of the order of a few picoamperes, and its duration is in the range of milliseconds to seconds, depending on channel subtype and on experimental conditions. Ion channels are opened transiently by specific ligands, by changing electric potentials or by lateral mechanical tension.

The latter is important for cell volume regulation and movement and may underlie the transduction of acousto-mechanic signals into electric potential variations at sensory hair cells of the inner ear (Morris, 1990; French, 1992). A correlation between mechanical excitation and electrical response at the level of single ion channels has not yet been possible. The SFM may offer this possibility, because forces in the piconewton range can be applied very locally and the site of force application can be controlled in the nanometer range by imaging the membrane structures under investigation. For such studies, a new type of patch clamp setup was

developed that includes an SFM to measure simultaneously mechanical and electrical properties of cell membranes with the SFM and the PCT.

With this step in the development of scanning probe instruments, the capability of microscopy to investigate the dynamics of biological processes of cell membranes under physiological conditions could be extended into the nanometer range. Presently, structures as small as about 10 nm can be resolved with either whole cells (Hörber et al., 1992) or excised membrane patches fixed to the pipette as described in this article.

Because the SFM probe applies forces to the plasma membrane under investigation the mechanical properties of cell surface structures contribute to the imaging process. On the one hand, topographic and elastic properties of the sample are represented in SFM images, whereas SFM provides information about the mechanical properties of cell membranes. The two aspects in the SFM images may be separated, for instance, by scanning forwards and backwards (Radmacher et al., 1992) or by scanning in the tapping mode (Benzanilla et al., 1994). Here we present measurements made in a combined SFM/PCT setup showing both the intracellular and the extracellular side of "excised" patches of plasma membrane. In addition, we describe preliminary results of measurements of the mechanical properties of inside-out patches.

MATERIALS AND METHODS

Experimental setup

A schematic representation of the combined SFM/PCT setup is shown in Fig. 1. The top and bottom of the bath chamber consist of two coverslips. Bath solution is kept between these slips by its surface tension. The chamber is about 15 mm in length, 8 mm in width, and 5 mm in height. Two sides of the chamber are open. The SFM cantilever is fixed at one edge of the chamber by a steel spring that is pressing against a ledge at the wall of the chamber by a screw. The laser beam (1 mW laser diode, λ = 670 nm) is set parallel to the length axis of the cantilever. It is focused by a collimator lens on the triangular shaped end of the cantilever. For all images shown, silicon nitride cantilevers are used that are 100 μm long and have a spring constant of 0.12 N/m (Park Scientific Instruments, Sunnyvale, CA), but also ultralevers of different producers were tested. The quadrant photo-detector
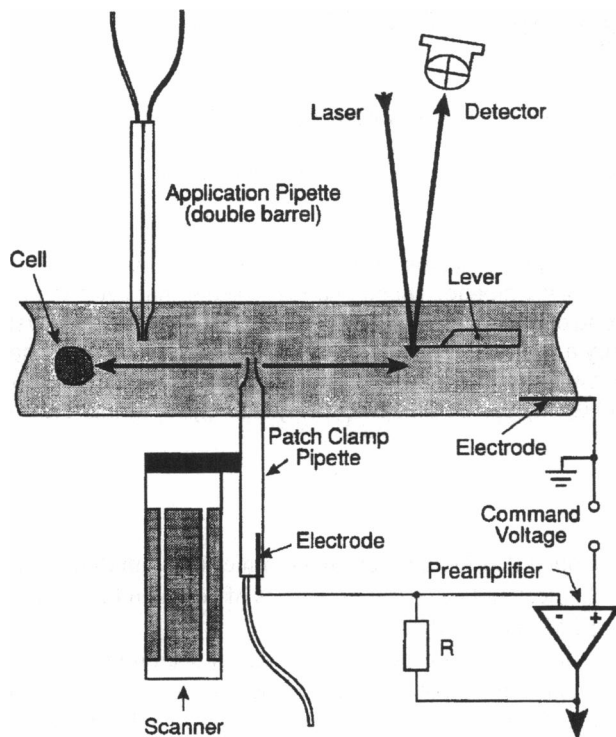
FIGURE 1   Schematic representation of the experimental setup used for the investigations of isolated membrane patches with a Scanning Force Microscope.

(5-mm^2 active surface) is covered by a 670-nm bandpass filter to reduce the effect of disturbing ambient light sources. Approximately half of the surface of the detector is illuminated by the laser beam. Both laser and detector are positioned at a distance of about 50 mm from the cantilever. They are adjustable in three dimensions by micrometer screws. A glass coverslip is placed at the position where the laser beam crosses the interface between air and bathing solution to prevent changes of beam direction because of fluctuations of the solution surface. The chamber, the double barrel pipette for fast application of chemical compounds, as well as the optical detection system are mounted on a motor controlled xyz manipulator.

The xyz manipulator holding the chamber and the optical system is fixed on a steel plate of 30-mm thickness. The inverted optical microscope for visual control can be moved independently by an xy stage. The quadrant piezo tube with a diameter of 10 mm and a wall thickness of 0.6 mm (Staveley Sensors, East Hartford, CT) is directly fixed to the steel plate insulated by a piece of macor. The scan width of the piezo tube was calibrated optically by interferometry. The pipette is fixed by a holder at the other end of the piezo tube such that it is held parallel to the piezo tube. The pipette holder was made of steel because of its mechanical properties, and its ability to shield the piezo by grounding the holder. Otherwise, the noise induced by the high voltages applied to the piezo ceramic during scanning would disturb the patch clamp current measurements. A glass coverslip between pipette holder and piezo tube was used to insulate the two parts. Because the patch pipette has to be moved by the piezo scanner in the SFM application, it could not be fixed on the head-stage of the PCT electronics by a standard pipette holder. We added a short silicon tube in between the pipette holder and the pipette to apply suction or pressure.

SFM imaging and patch-clamp recording

All imaging was done with the scan direction set parallel to the axis of the lever. Scan rates ranged from 100 Hz to 1 kHz, and loading forces were set as low as possible (<1 nN). SFM data were recorded on video tape with the

help of a PC-video card. Image analysis was performed off-line on a Silicon Graphics computer after digitizing the video signal by a frame grabber card.

PCT data were measured with an EPC7 amplifier (List, Darmstadt, Germany), filtered at 3 kHz by a Bessel filter, digitized by an ITC 16 D/A converter (Instrutech, Elmont, NY), and stored on a MacIntosh fx computer.

Sample preparation

Oocytes were harvested from adult *Xenopus laevis* under anesthesia (0.1% aminobenzoic acid ethylester (Sigma Chemical Co., St. Louis, MO)) and manually dissected. They were incubated at 19°C in modified Barth's solution containing penicillin and streptomycin (100 units/ml). The follicle layers of the oocytes were removed by incubating in modified Barth's solution containing collagenase type II (Sigma, 1 mg/ml). Before the experiments, the vitelline membrane was removed mechanically after incubating the oocyte in a hyperosmolar solution to induce shrinkage (Methfessel et al., 1986). The skinned oocyte was placed in the bath chamber on the bottom coverslip, and solution flow was stopped for 5 min to allow the oocyte to adhere firmly to the plastic.

Pipettes were pulled from thick wall (0.5 mm) or thin wall (0.3 mm) borosilicate glass (outer diameter 2 mm) to a final tip diameter of about 2 μm. They were back-filled with the same solution that was used for bath chamber perfusion containing (in mM): 100 KCl, 10 HEPES, 10 EGTA, 2 MgCl$_2$, pH 7.2 (KOH).

GΩ-Seal formation (Fig. 2) was carried out as described previously (Hamill et al., 1981), but without suction to keep the membrane at the end of the pipette. The isolated inside-out, outside-out, and vesicle patches were positioned in front of the tip of the SFM cantilever by a motor-driven xyz stage under the control of the optical microscope.

RESULTS AND DISCUSSION

Comparison between inside and outside of the patch membrane

For SFM observations, the vesicles formed inside the patch pipette turned out to be the most stable type of membrane preparation. These membranes could be observed for hours, and application of positive or negative pressure or electric field did not destroy them. They could be moved several
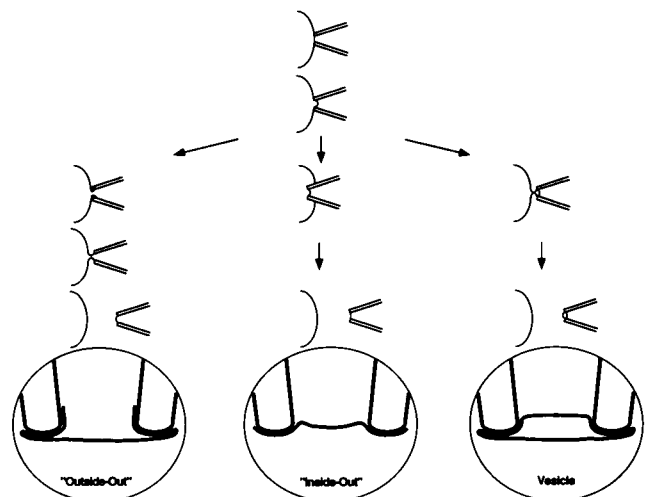

FIGURE 2   Schematic representation of procedure for forming excised membrane patches spanning the tip of a glass pipette (modified from Hamill et al., 1981). Magnifications show the shapes of the patch preparations as suggested by our experiments.

micrometers by the application of suction or pressure, maintaining the GΩ resistance contact between the glass wall and membrane.

Outside-out patches were less stable and were destroyed frequently when the pipette approaches the cantilever; they were probably cut by the edges of the triangular shaped silicon nitride cantilever or by the edges of the pyramidal tip, because this type of membrane preparation is thought to protrude in the form of an Ω out of the end of the pipette tip (Fig. 2).

Inside-out patches were more stable than outside-out patches and were protected better because they lie more toward the inside of the pipette. Nevertheless, if they were formed by applying weak suction they could be observed by
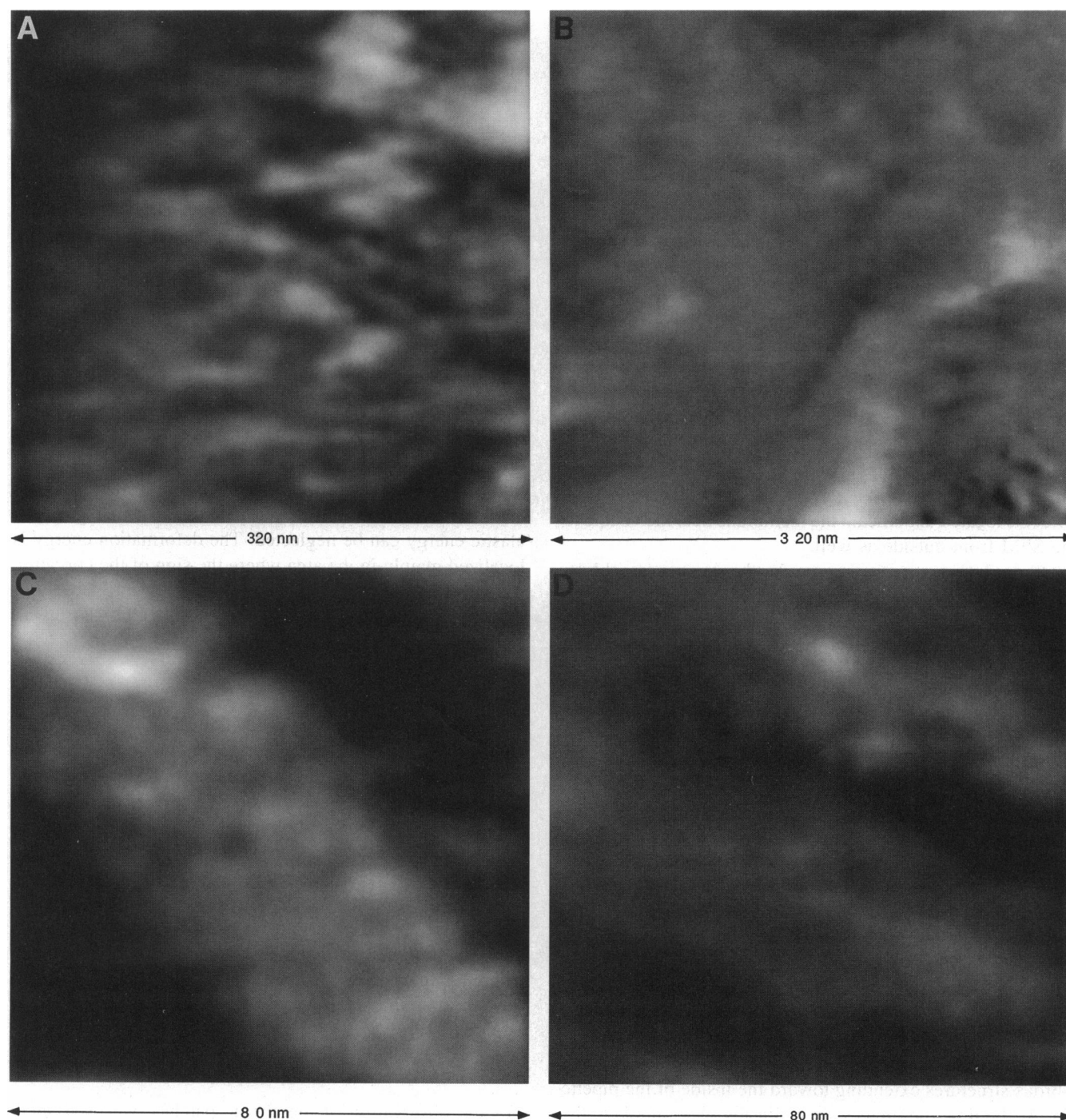

FIGURE 3   Comparison of cytoplasmic and extracellular surface of the plasma membrane as seen on an inside-out patch or a vesicle fixed at the tip of a patch pipette. Images shown are stable during repetitive scanning. Changes can be induced by application of pressure to the pipette or changing the loading force of the cantilever. (A) Image of an inside-out patch in the center of the pipette tip. (B) Image of the outer side of the membrane of a vesicle. (C) Detailed image of a fibrous structure on an inside-out patch. (D) Fibrous structures imaged from the outer side of the membrane.

the SFM (Fig. 2). The pyramidal tip of the cantilever, that is about 4 μm long and has a basis area of about 5 × 5 μm^2, cannot go too far into the pipette opening of about 1 μm in diameter. Cantilevers with sharper tips, like the so-called ultralevers, would probably be more adequate for this preparation, but they get destroyed by the glass wall of the pipette during the approach very easily.

Images of membrane patches obtained with different types of cantilevers show that their common structural feature is that of fibers extending from the glass wall toward the center of the patch. This gives the membrane patch the appearance of a tent stabilized by a scaffold of ropes. Fig. 3 compares the structures observed on the inside (Fig. 3 A) and the outside (Fig. 3 B) of the oocyte plasma membrane fixed to the patch pipette as either an inside-out patch or as a vesicle. On smaller scan areas shown in Fig. 3, C and D, the fibrous structures can be imaged more clearly with details smaller than 10 nm on inside-out patches.

These structures are comparable in size and arrangement with what was observed in membrane preparations on solid supports with the STM (Ruppersberg et al., 1989). The most likely interpretation of the nature of these fibers is that they are part of the cytoskeleton located directly underneath the plasma membrane. These structures are known to be constructed by an actin fiber network connected tightly to membrane proteins. They stabilize the membrane from the cytoplasmic side. As the cantilever tip applies a force onto the membrane, the topographic and elastic information is combined in SFM images in a way that these cytoskeleton constituents located underneath the membrane become visible to the SFM from outside as well.

Other, larger structures seen in the images are blobs and rings of 10–100 nm size that are arranged along the fibers. Although their molecular constituents are not yet clear, it is likely with the present resolution that the combined SFM/PCT setup provides a tool for further studies of these structures, for instance, by in situ application of affinity reagents.

Attachment of the membrane to the pipette glass

One question often raised when patch clamp techniques are used is: how are membranes fixed to the glass of the pipette to form the high resistance "seals" (GΩ-seal) (Milton et al., 1990; Zuazaga et al., 1990)? Fig. 4 A shows remnants of a broken outside-out patch remaining on the pipette glass rim together with fiber structures of the cytoskeleton. Fibers are still fixed to the rim together with blobs up to 100 nm in size that are oriented with respect to the fibers, as shown in detail in Fig. 4 B. Fig. 4, C and D show similar structures of another broken outside-out patch that exhibits other types of large fibrous structures extending toward the inside of the pipette tip. At the time the images shown in Fig. 4 were taken, the pipette access resistance had already dropped to the value close to the resistance of the open pipette (2 MΩ), indicating the removal of the membrane from the pipette tip. These observations are consistent with results on preparations of

lipids and proteins on surfaces for STM and SFM studies, where proteins can attach more firmly to the surface than lipids (Hörber et al., 1988).

It seems likely, therefore, that these proteins are necessary for the binding of the membrane to the glass wall to form the GΩ-seal. One possibility arising from the observations with SFM of membrane patches is that the lipids act like a viscous glue responsible for sealing. In addition, the internal lipid interaction forces can help to stabilize the membrane structure, but the essential role is played by cytoskeleton structures.

Membrane elasticity

The stiffness of the membrane can be seen in experiments with a negative pressure of 25 mbar applied to the inside of the pipette. Only the central part of an inside-out patch, 500 nm in diameter, moves toward the inside of the pipette (Fig. 5). This indicates a high stiffness of the membrane patch. The excised membrane can be considered as a bowl with very thin walls and fixed ends (Fig. 6). The radius R of the bowl can be estimated to be about 1 μm by the movement of the piezo in the direction perpendicular to the membrane while scanning over the membrane from one side of the glass rim to the other. The energy of a deformation δx of a membrane with thickness h and elasticity coefficient E per area is in this case proportional to $Eh(\delta x/R)^2$, and the elastic energy is proportional to $Eh^3(\delta x/R^2)^2$. This means that if a deformation occurs as in the case of the inside-out patch shown in Fig. 5, the elastic energy can be neglected. The deformation energy is localized mainly in the area where the sign of the curvature changes. The depth of the intrusion, H, is correlated to a uniformly applied pressure p according to Landau et al. (1975) by

$$H \sim h^5 E^2/R^4 p^2. \tag{1}$$

If, as in the membrane patch shown in Fig. 5, negative pressure of 25 mbar is applied, the deformation observed (about 150 nm) can be used for a rough estimate of the membrane thickness h and the elasticity coefficient E. E has to be 0.5 × 10^9 N/m^2 to obtain a thickness of 5 nm for the patch membrane. If E is assumed to be 0.1 × 10^9 N/m^2, the thickness would be 10 nm according to Eq. 1.

With the SFM, forces can also be applied very locally onto the membrane patch with the tip of the cantilever. In this case, the deformation depth is correlated in a different way to the applied force f because it is not acting uniformly on the whole membrane. According to Landau et al. (1975), it is given by

$$H \sim f^2 R^2/E^2 h^5. \tag{2}$$

For the observation of membrane patches, we used small forces below 1 nN. At 1 nN, signs of a deformation of the membrane occurred that were about 10 nm measured with respect to the glass rim. With these values, the elasticity coefficient E can be estimated by Eq. 2 to be 5 × 10^9 N/m^2,
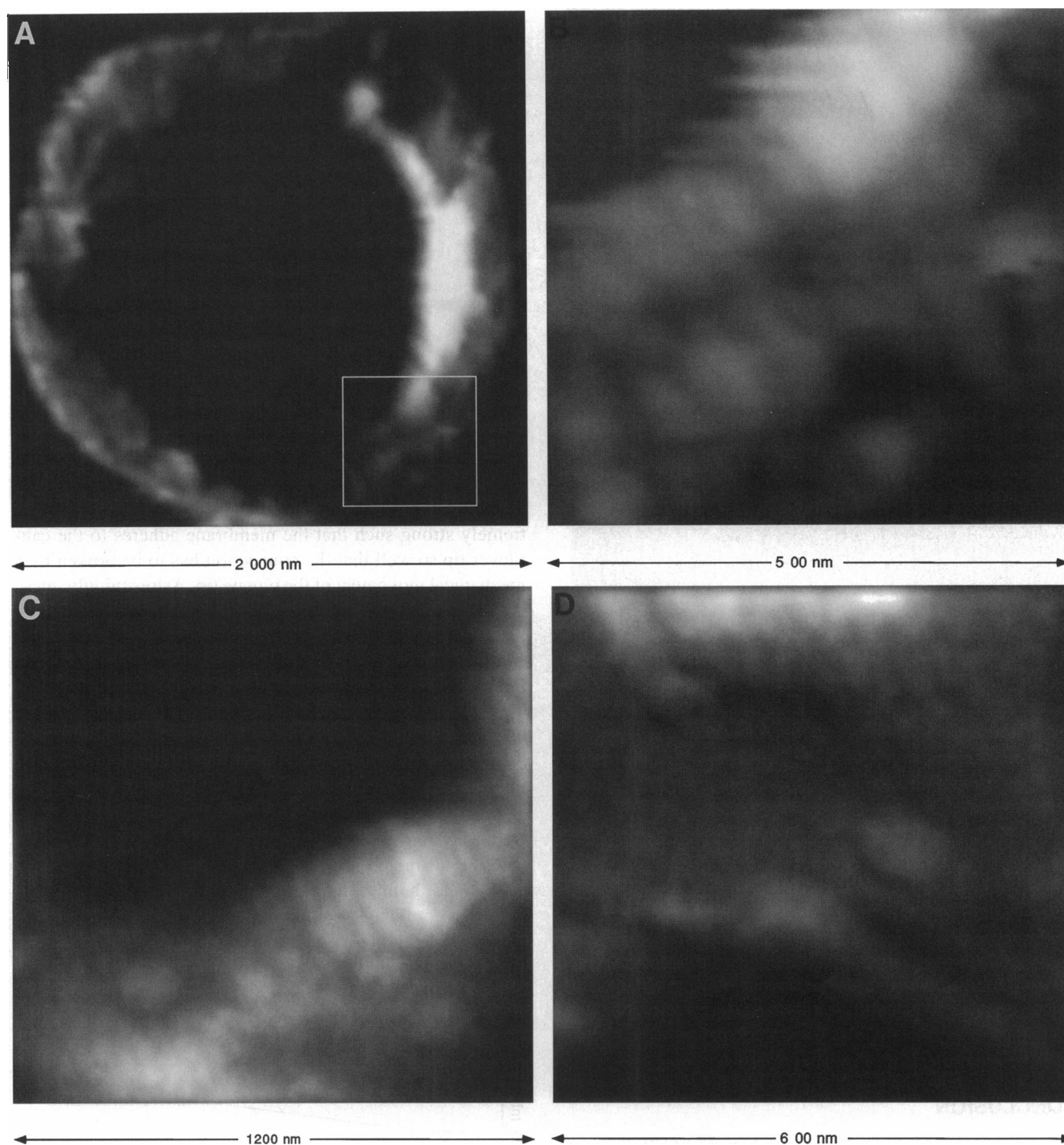
FIGURE 4   Parts of oocyte plasma membrane attached to the tip of the pipette. (A) Tip of the glass pipette with remnants of an outside-out patch. (B) Details on the glass rim of the same pipette as shown in A (□). (C) Circular impressions seen on the remnant membrane on the top of the pipette rim. (D) Magnified view of the membrane with fibrous structures pointing toward the inside of the pipette.

if the thickness of the membrane is assumed to be 5 nm. When negative pressure is applied to the pipette, the membrane-glass attachment is more closely involved in the elastic response of the membrane than for the very local application of a force by the cantilever tip. The weaker intermolecular forces between glass and membrane possibly lead to the apparent smaller elasticity in the experiments with

application of negative pressure. With both approaches, the value of the membrane elasticity lies in between the values known for fiber-reinforced polypropylene (2.5–6×10^9 N/m^2) and polyethylene (0.15–1.5×10^9 N/m^2), which is two to three orders of magnitude lower than the elasticity coefficient of steel (196×10^9 N/m^2) (Stöcker, 1994). These results give spring constants that are about 30 times higher
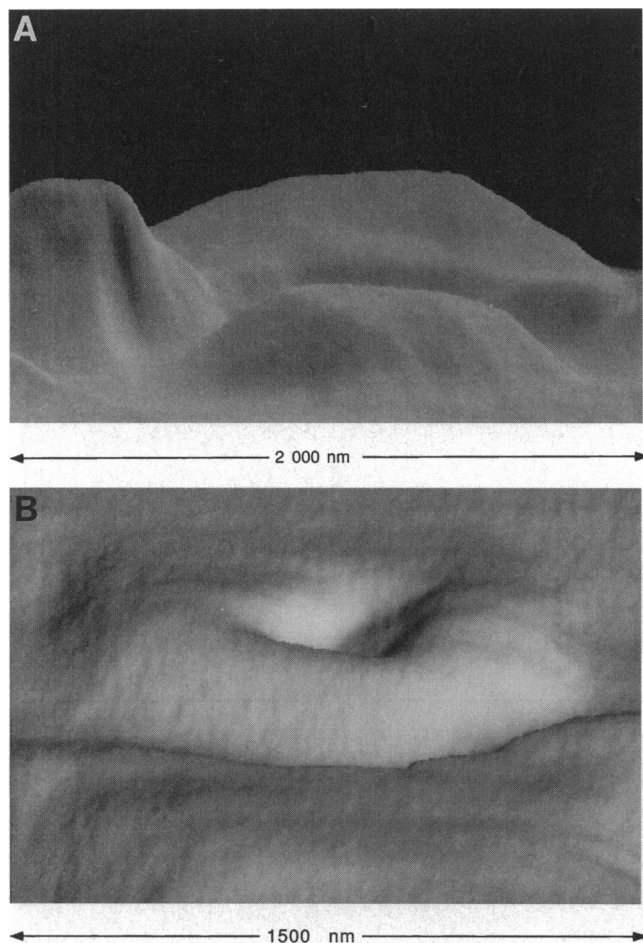
FIGURE 5   Deformation of an inside-out patch by application of 25-mbar negative pressure inside the pipette. (A) Image of the patch at zero pressure. The higher parts in the background are part of the pipette tip. The patch appears as a smooth structure in the middle of the image. (B) Image of the patch during application of negative pressure. The rim of the pipette is in the foreground of the image. Application of negative pressure moved the central part of the inside-out patch into the pipette. Two different image processing procedures were used for the pictures shown.

than those determined on living MDCK cells on glass (Hoh et al., 1994). This points to an interesting difference between intact cells and excised membrane patches.

CONCLUSION

These first experiments with the combined SFM/PCT setup are still very qualitative, but they clearly show the potential of this technique for studying membrane structure. For more quantitative analyses in the future, the interaction forces between cantilever tip and membrane have to be studied in more detail. These forces are surely small enough, on average, to give a good representation of the deformation generated by the application of pressure, suction, or electric field forces to the membrane. Interaction forces between cantilever tip and membrane can also be used to apply forces locally from the piconewton up to the micronewton range.

With inside-out patches, the attractive forces between cantilever tip and membrane can become, in certain places, ex-
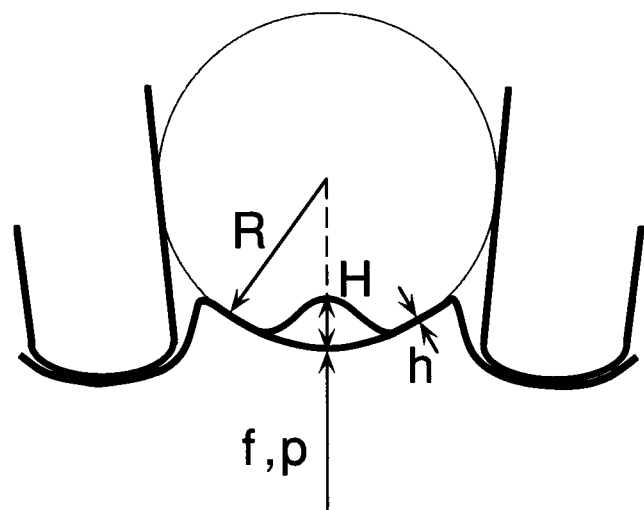

FIGURE 6   Schematic drawing of an inside-out patch at the tip of a glass pipette with the symbols used in the text.

tremely strong such that the membrane adheres to the cantilever tip so well that the connection has to be broken by a mechanical movement of the pipette tip. Astonishingly, these manipulations, in most cases, destroy neither the membrane patch nor the $G\Omega$-seal between membrane and glass, indicating a much greater flexibility of the membrane patch than indicated in the experiments with application of pressure. This is an interesting aspect for future experiments, which will also have to investigate the time dependence of the mechanical reaction of the membrane to applied forces. With the high resonance frequency of 7 kHz and long term stability of 100 nm/h drift of the setup, this is possible over a useful frequency range.

As in all membrane patches, cytoskeleton structures are visible and the investigation of mechanogated ion channels with this combined setup should also be possible, because these cytoskeleton parts, which are fixed directly to the membrane, seem to be essential for the activation of mechanogated ion channels (Morris, 1990; Hamill et al., 1992). In our initial experiments with native mechanogated ion channels of
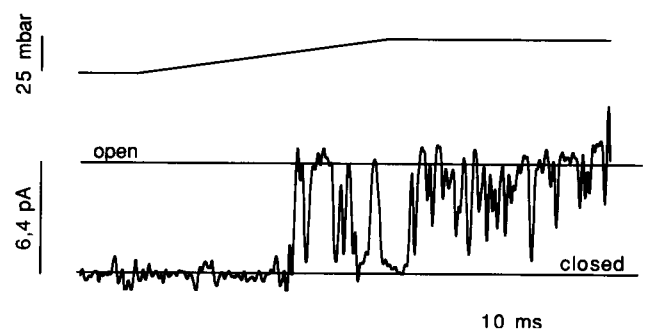

FIGURE 7   The opening of endogenous mechanosensitive ion channels of *X. laevis* oocytes evoked by application of 25-mbar negative pressure to an isolated outside-out patch. Holding potential was +120 mV, and patch current was filtered at 1 kHz. The upper trace shows schematically time course of pressure application.

oocyte membranes, only the frequency of occurrence of opening events could be influenced with pressure applied to the pipette or force applied with the cantilever (Fig. 7). With different types of cells or by expressing recombinant mechanosensitve ion channels, this possibly could be done at the single-channel level. The combination of the two techniques may lead to a variety of new applications of the patch-clamp technique in studies of membrane structures and properties that are necessary to understand processes such as hearing or touching and a variety of other functions, including cell volume regulation.

REFERENCES

Benzanilla, M., B. Drake, E. Nudler, M. Kashlev, P. K. Hansma, and H. G. Hansma. 1994. Motion and Enzymatic Degradation of DNA in the Atomic Force Microscope. *Biophys. J.* 67:2454–2459.

Chang, L., T. Kious, M. Yorgancioglu, D. Keller, and J. Pfeifer. 1993. Cytoskeleton of living, unstained cells imaged by scanning force microscopy. *Biophys. J.* 64:1282–1286.

French, A. S. 1992. Mechanotransduction. *Annu. Rev. Physiol.* 54:135–152.

Häberle, W., J. K. H. Hörber, and G. Binnig. 1989. Force Microscopy on Living Cells. *J. Vac. Sci. Technol.* B9:1210–1212.

Hamill, O. P., A. Marty, E. Neher, B. Sakmann, and F. J. Sigworth. 1981. Improved patch-clamp techniques for high-resolution current recording from cells and cell-free membrane patches. *Pflügers Arch.* 391:85–100.

Hamill, O. P., and D. W. J. McBride. 1992. Rapid adaptation of single mechanosensitive channels in *Xenopus* oocytes. *Proc. Natl. Acad. Sci. USA.* 89:7462–7466.

Henderson, E., P. G. Haydon, and D. S. Sakaguchi. 1992. Actin Filament Dynamics in Living Glial Cells Imaged by Atomic Force Microscopy. *Science* 257:1944–1946.

Hoh, J. H., and P. K. Hansma. 1992. Atomic Force Microscopy for High Resolution Imaging in Cell Biology. *Trends Cell Biol.* 7:208–213.

Hoh, J. H., and C.-A. Schoenenberger. 1994. Surface morphology and mechanical properties of MDCK monolayers by atomic force microscopy. *J. Cell Sci.* 107:1105–1114.

Hörber, J. K. H. 1992. Investigation of living cells in the nanometer regime with the scanning force microscope. *Scanning Microsc.* 6:919–29.

Hörber, J. K. H., C. A. Lang, T. W. Hänsch, W. M. Heckl, and M. H. 1988. Scanning tunneling microscopy of lipid films and embedded biomolecules. *Chem. Phys. Lett.* 145:151–154.

Landau, L. D., and E. M. Lifshitz. 1975. Lehrbuch der Theoretischen Physik. VII. Elastizitäts-Theorie. Akademie Verlag, Verlag, Berlin.

Le Grimellec, C., E. Lesniewska, C. Cachia, J. P. Schreiber, F. de Fornel, and J. P. Goudonnet. 1994. Imaging of the Membrane Surface of MDCK Cells by Atomic Force Microscopy. *Biophys. J.* 67:36–41.

Methfessel, C., V. Witzemann, T. Takahashi, M. Mishina, S. Numa, and B. Sakmann. 1986. Patch clamp measurements on *Xenopus laevis* oocytes: currents through endogenous channels and implanted acetylcholine receptor and sodium channels. *Pflügers Arch.* 407:577–588.

Milton, R. L., and J. H. Caldwell. 1990. How do patch clamp seals form? *Eur. J. Physiol.* 416:758–765.

Morris, C. 1990. Mechanosensitive ion channels. *J. Membr. Biol.* 113:93–107.

Radmacher, M., R. W. Tillamnn, M. Fritz, and H. E. Gaub. 1992. From molecules to cells: imaging soft samples with the atomic force microscope. *Science.* 257:1900–1905.

Ruppersberg, J. P., J. K. H. Hörber, C. Gerber, and G. Binnig. 1989. Imaging of cell membranous and cytoskeleton structures with a scanning tunneling microscope. *FEBS Lett.* 257:460–464.

Stöcker, H. 1994. Taschenbuch der Physik. Harry Deutsch Verlag, Thun und Frankfurt/Main.

Zuazaga, C., and A. Steinacker. 1990. Patch-clamp recording of ion channels: interfering effects of patch pipette glass. *NIPS.* 5:155–158.